Transition Met Chem (2016) 41:97–105
DOI 10.1007/s11243-015-0001-8

Catalytic behavior of an iron(III) complex containing an N,O-type bidentate oxazoline ligand for selective oxidation of sulfides

Mojtaba Amini[1] · Mostafa Khaksar[2] · Ali Arab[3] · Reza Masoomi Jahandizi[4] · Mojtaba Bagherzadeh[2] · Davar M. Boghaei[2] · Arkady Ellern[5] · L. Keith Woo[5]

Received: 12 September 2015 / Accepted: 5 November 2015 / Published online: 14 November 2015
© Springer International Publishing Switzerland 2015

Abstract The reaction of $Fe(acac)_3$ and 2-(2′-hydroxyphenyl)oxazoline (Hphox) as a bidentate O,N donor ligand afforded a six-coordinated iron(III) complex $[Fe(phox)_2(acac)]$ with distorted octahedral configuration. The complex was isolated as an air-stable crystalline solid and characterized by elemental analysis, FTIR, solution electrical conductivity, and by single-crystal X-ray structure analysis. The structure, electronic properties, and vibrational normal modes of the complex were investigated by DFT. The use of this complex as a catalyst for the oxidation of sulfides to their corresponding sulfoxides using urea hydrogen peroxide as the primary oxidant was investigated. The catalyst shows very efficient reactivity, giving high yields and selectivities at room temperature under air.

✉ Mojtaba Amini
mamini@maragheh.ac.ir

1 Department of Chemistry, Faculty of Science, University of Maragheh, P.O. Box. 55181-83111, Maragheh, Iran

2 Chemistry Department, Sharif University of Technology, P.O. Box 11155-3615, Tehran, Iran

3 Department of Chemistry, Semnan University, P.O. Box. 35131-19111, Semnan, Iran

4 Department of Biology, Faculty of Science, University of Maragheh, Maragheh, Iran

5 Chemistry Department, Iowa State University, Ames, IA 50011-3111, USA

Introduction

Selective oxidation of sulfides to sulfoxides is an essential step in many biological and industrial processes. The resulting sulfoxides are essential intermediates for a number of applications. A number of methods have been developed for the conversion of sulfides into sulfoxides [1–4]. Iron compounds are not only low cost and environmentally friendly, but also used by nature in a variety of metalloenzymes and especially in oxidation reactions. Thus, in the last two decades, considerable effort has been invested in the search for synthetic iron catalysts with various ligands to promote oxidation reactions [5–8].

Compounds containing an oxazoline ring have become one of the most successful, versatile, and commonly used classes of ligands for catalysis of various reactions, due to their accessibility from readily available amino alcohols in short and high yielding syntheses, as well as their modular nature and applicability in a wide range of metal-catalyzed transformations [9–11]. Many complexes of such ligands show excellent catalytic activity, and there have been many recent reports on their applications in homogeneous and heterogeneous catalysis [12–14].

Density functional theory (DFT) has been widely used in the prediction of structure, electronic properties, and spectroscopic properties of metal complexes [15–17]. Electron transfer process in iron complexes with cyanide, pyrazine, 4,4′-bipyridine, and azide ligands has been studied by the B3LYP hybrid density functional method [15]. Jaworska et al. [16] have investigated the electronic structures and UV–Vis spectra of iron complexes with EDTA and NO ligands using the B3LYP functional. Conradie et al. [17] have employed DFT calculations using different functionals in order to study the properties of isomers of tris(beta-diketonato)$_3$ iron complexes, and their

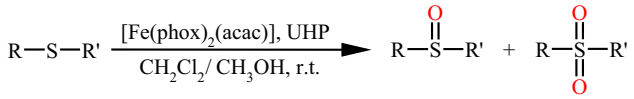

Scheme 1 Oxidation of sulfides by the $[Fe(phox)_2(acac)]$/UHP catalytic system

results showed that the B3LYP functional provides the best description of both the spin state and geometry of such complexes.

Continuing our studies on the oxidation of sulfides using five-coordinated iron(III) complexes with ligands based on oxazoline, oxazine, and thiazoline rings [18–20], herein we describe the synthesis of a new six-coordinated Fe(III) complex $[Fe(phox)_2(acac)]$ (Hphox = 2-(2′-hydroxyphenyl)oxazoline and acac = acetylacetonate). The complex has been characterized by X-ray crystallography as well as DFT calculations and examined as a catalyst in the oxidation of sulfides in the presence of urea hydrogen peroxide (UHP) as an oxidant under air at room temperature (Scheme 1).

Experimental section

General procedures

Chemicals and solvents were purchased from Fluka and Merck. 2-(2′-Hydroxyphenyl)oxazoline (Hphox) was synthesized according to a published procedure [21].

Elemental analyses (C, H, N) were obtained with a Carlo ERBA Model EA 1108 analyzer. FTIR spectra were obtained with a Unicam Matson 1000 FTIR spectrophotometer using KBr disks at room temperature. Molar conductances were determined in methanol (ca. 10^{-3} M) at room temperature using a Toa CM 405 conductivity meter. The products of oxidation reactions were determined and analyzed with an HP Agilent 6890 gas chromatograph equipped with a HP-5 capillary column and flame ionization detector.

Synthesis of the complex

To a solution of $Fe(acac)_3$ (0.353 g, 1.00 mmol) in ethanol (15 mL) was added a solution of 2-(2′-hydroxyphenyl) oxazoline and (0.326 g, 2.00 mmol) of the ethanol (10 mL). After stirring at room temperature for 4 h, the solution was filtered and evaporated under reduced pressure to give a precipitate. Recrystallization from acetonitrile yielded the complex as dark brown crystals. Yield: 0.361 g, 75 %. Anal. Calcd for C23H23FeN2O6: C, 57.6; H, 4.8; N, 5.8. Found: C, 57.5; H, 4.8; N, 5.9 %. Selected IR frequency (KBr disk, cm^{-1}): 1611 ($\nu_{C=N}$); Λ_M (Ω^{-1} cm^2 mol^{-1}): 11.5.

General procedure for sulfide oxidation

The following standard procedure was used for sulfide oxidation experiments. To a solution of sulfide (0.2 mmol), chlorobenzene (0.2 mmol) as internal standard and $[Fe(phox)_2(acac)]$ (0.01 mmol) in a 1:1 mixture of CH_3OH/CH_2Cl_2 (1 mL), was added UHP (0.4 mmol). The mixture was stirred at room temperature, and the reaction progress was monitored by GC. Products were identified by comparison with authentic samples.

X-ray crystallography

The crystal evaluation and data collection were performed on the Bruker SAINT Software package using a narrow-frame algorithm. A red block-like crystal of $C_{23}H_{23}FeN_2O_6$, approximate dimensions 0.090 mm × 0.170 mm × 0.700 mm, was used for the X-ray crystallographic analysis. The frames were integrated with the Bruker SAINT software package using a narrow-frame algorithm. The integration of the data using a monoclinic unit cell yielded a total of 23118 reflections to a maximum θ angle of 25.25° (0.83 Å resolution), of which 3941 were independent (average redundancy 5.866, completeness = 99.5 %, R_{int} = 9.15 %) and 2560 (64.96 %) were $>2\sigma(F^2)$. The final cell constants of a = 11.809(2) Å, b = 14.117(3) Å, c = 13.887(3) Å, β = 108.789(3)°, and volume = 2191.7(7) $Å^3$ are based upon the refinement of the XYZ-centroids of 2674 reflections above 20 $\sigma(I)$ with $4.647° < 2\theta < 43.13°$. Data were corrected for absorption effects using the multi-scan method (SADABS). The ratio of minimum to maximum apparent transmission was 0.851. The calculated minimum and maximum transmission coefficients (based on crystal size) were 0.6290 and 0.9370. The final anisotropic full-matrix least-squares refinement on F^2 with 291 variables converged at R_1 = 4.55 %, for the observed data and wR_2 = 12.05 % for all data. The goodness-of-fit was 1.007. The largest peak in the final difference electron density synthesis was 0.503 $e^-/Å^3$, and the largest hole was −0.437 $e^-/Å^3$ with an RMS deviation of 0.066 $e^-/Å^3$. On the basis of the final model, the calculated density was 1.452 g/cm^3 and $F(000)$, 996 e^-.

Computational methods

The structure of the complex was geometry-optimized using the B3LYP hybrid density functional and 6−31+G* basis set. A frequency calculation was performed on the optimized structure in order to confirm that it was a local minimum on the potential energy surface. All calculations were performed using the Gaussian03 program [22].

Results and discussion

Complex characterization

The complex was obtained by the reaction of two equivalents of 2-(2′-hydroxyphenyl) oxazoline with one equivalent of $Fe(acac)_3$ (Scheme 2). The fast color change from cherry red to a dark brown solution during the synthesis indicated coordination of ligand.

The new iron(III) complex is dark brown, stable in air and light and soluble in methanol, ethanol, acetonitrile, methylene chloride, DMF, and DMSO. The elemental analyses and spectroscopic data for the complex agree very well with its formulation as $[Fe(phox)_2(acac)]$.

In order to study the binding mode of the oxazoline ligand, the IR spectrum of free Hphox was compared with the spectrum of the complex. The shift of the band assigned to C=N from 1624 (free ligand) to 1611 cm^{-1} (complex) indicates coordination of the azomethine nitrogen to iron [23, 24].

The molar conductivity of the complex in methanol was 11.5 Ω^{-1} cm^2 mol^{-1}, indicating a non-electrolytic nature [25].

The structure of the complex has been determined by X-ray crystallography, and an ORTEP view of the complex with atom numbering scheme is shown in Fig. 1. A suitable single crystal of the complex was obtained by slow evaporation from MeCN solution. A summary of the X-ray structure refinement is shown in Table 1, and a crystal packing diagram of the complex is shown in Fig. 2.

The complex crystallizes in the monoclinic crystal system and space group *P* 1 21/n 1 and has a tetragonally compressed octahedral FeN_2O_4 chromophore. The iron atom is ligated by four donor atoms [N(1), N(2), O(2) and O(4)] from two chelating phox ligands plus two oxygen atoms [O(5) and O(6)] of one acac ligand. The complex is mononuclear, consisting of discrete monomeric units of $[Fe(phox)_2(acac)]$, in which the acetate ligand is in an all-equatorial position, with bond distances of 2.014(3) and 2.030(3) Å for Fe_1–O_5 and Fe_1–O_6, respectively, while the two donor atoms of each oxazoline ligand occupy one equatorial and one axial position. The rather short Fe_1–O_2 and Fe_1–O_4 distances of 1.934(2) and 1.951(2) Å compared to the equatorial coordination distances are indications of tetragonal compression [26].

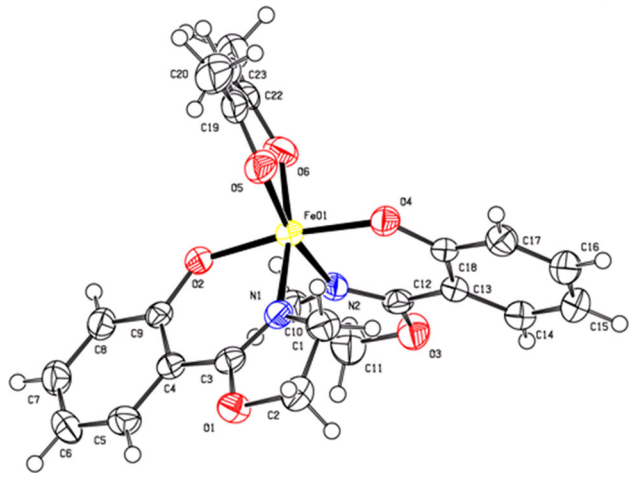

Fig. 1 ORTEP diagram of the complex $[Fe(phox)_2(acac)]$ with thermal ellipsoids drawn at a 50 % probability limit

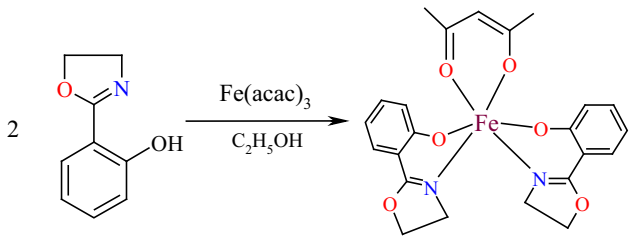

Scheme 2 Synthesis of $[Fe(phox)_2(acac)]$

DFT results

The geometry-optimized structure of the complex obtained from DFT calculations has a distorted octahedral configuration, in accordance with the X-ray crystallographic analysis. Table 2 presents some selected calculated and experimental bond lengths and bond angles for the complex. The calculated bond lengths are almost all slightly shorter than the corresponding experimental values. The error is in the 2–7 % range for Fe–O(N) bond lengths and <1 % for other bond lengths. Both shorter and longer calculated bond lengths, compared to experimental values, have been reported previously [27–29]. The differences have been attributed to environmental effects as well as the choice of DFT method [27–29].

The calculated natural bond orbital (NBO) atomic charge on Fe_1 is +0.717, while those on O1, O2, O3, O4, O5, O6, N_1, and N_2 are −0.529, −0.592, −0.529, −0.592, −0.573, −0.573, −0.443, and −0.443, respectively. The charge on the iron atom is thus significantly lower than the formal charge of +3 indicating charge transfer from the ligands to the metal center. Figure 3 shows the HOMO−1 (−5.06 eV), HOMO (−5.59 eV), LUMO (−1.38 eV), and LUMO+1 (−1.28 eV) of the complex. It is clear that while the HOMO-1 and HOMO orbitals show smaller contributions on Fe, the LUMO and LUMO+1 orbitals show greater contributions on and around the Fe atom. The calculated HOMO–LUMO energy gap is 4.21 eV, indicating good stability and chemical hardness of the complex.

Table 1 Crystal data and structure refinement for complex [Fe(phox)$_2$(acac)]

	[Fe(phox)$_2$(acac)]
Empirical formula	$C_{23}H_{23}FeN_2O_6$
Formula weight	479.28
Temperature	173 (2) K
Wavelength	0.71073 Å
Crystal system	Monoclinic
Space group	*P* 1 21/*n* 1
Unit cell dimensions	$a = 11.809(2)$ Å
	$\alpha = 90°$
	$b = 14.117$ (3) Å
	$\beta = 108.789$ (3)°
	$c = 13.887$ (3) Å
	$\gamma = 90°$
Volume	2191.7 (7) Å^3
Z	4
Density (calculated)	1.452 g/cm^3
Absorption coefficient	0.731 mm^{-1}
F(000)	996
Crystal size	0.090 × 0.170 × 0.700 mm
Theta range for data collection	1.98 to 25.25°
Index ranges	$-14 \le h \le 14$, $-16 \le k \le 16$, $-16 \le l \le 16$
Reflections collected	23118
Independent reflections	3941 [R(int) = 0.0915]
Completeness to theta = 28.70°	99.5 %
Absorption correction	Multi-scan
Maximum and minimum transmission	0.9370 and 0.6290
Refinement method	Full-matrix least-squares on F^2
Data/restraints/parameters	3941/0/291
Goodness of fit on F^2	1.007
Final R indices [$I > 2\Sigma(I)$]	$R_1 = 0.0455$, w$R_2 = 0.1018$
R indices (all data)	$R_1 = 0.0900$, w$R_2 = 0.1205$
Largest difference peak and hole	0.503 and −0.437eÅ^{-3}

$R_{int} = \Sigma|F_o2-F_o2(\text{mean})|/\Sigma[F_o2]$

$R_1 = \Sigma||F_o|-|F_c||/\Sigma|F_o|$

GOOF = $S = \{\Sigma[w(F_o2-F_c2)2]/(n-p)\}1/2$

w$R_2 = \{\Sigma[w(F_o2-F_c2)2]/\Sigma[w(F_o2)2]\}1/2$

$w = 1/[\sigma(F_o2) + (\text{aP})2 + \text{bP}]$ where P is $[2F_c2 + \text{Max}(F_o2, 0)]/3$

A frequency calculation on the complex at the B3LYP/6-31G* level of theory confirmed that the optimized structure is a minimum on the potential energy surface. Some of the experimental and corresponding calculated vibrational frequencies along with the probable assignments are reported in Table 3. It should be added that the calculated vibrational frequencies have been scaled by a factor of 0.9613 in order to correct for theoretical errors such as electron correlation and basis set deficiencies [30]. Good agreement between experimental and calculated vibrational frequencies is observed. According to the computational results, vibrations in the region of 3093–3054 cm^{-1} are related to the aromatic C–H stretching of benzene groups in agreement with the results reported in the literature [31]. Vibrations in the region of 3035–2936 cm^{-1} are related to the C–H stretching modes of the oxazoline and acac rings. The calculated C=N stretching frequency of the complex is 1610 cm^{-1}, in very good agreement with the experimental value of 1611 cm^{-1}. The aromatic C–H in-plane and out-of-plane bending modes of benzene and its derivatives have been reported in the region of 1300–1000 and 1000–675 cm^{-1}, respectively [32]. Our calculated frequencies for the aromatic C–H in-plane bending and C–H out-of-plane bending

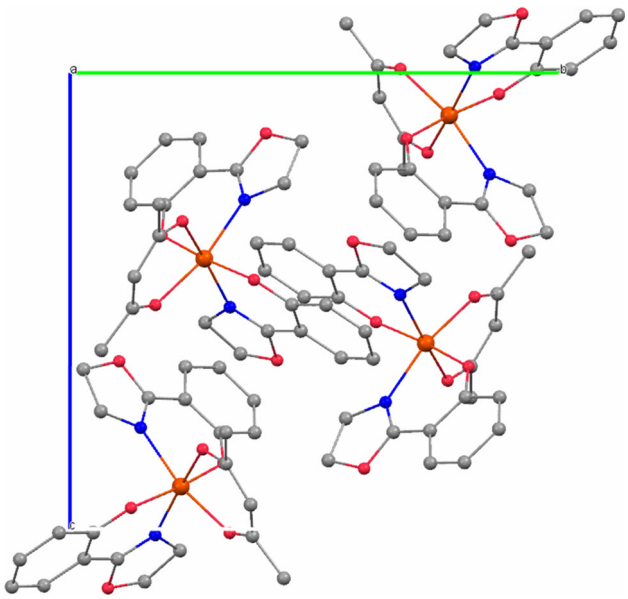

Fig. 2 Crystal packing diagram of the complex [Fe(phox)$_2$(acac)]

Table 2 Observed (X-ray) and calculated (DFT) geometrical parameters for the complex

Bond	DFT (Å)	X-ray (Å)	Angle	DFT (°)	X-ray (°)
Fe_1–O_2	1.897	1.934(2)	O_2–Fe_1–O_4	175.46	171.06(10)
Fe_1–O_4	1.897	1.951(2)	N_1–Fe_1–O_6	177.59	168.92(11)
Fe_1–O_5	1.945	2.014(3)	N_2–Fe_1–O_5	177.59	168.03(11)
Fe_1–O_6	1.945	2.030(3)	O_5–Fe_1–O_6	93.07	85.89(11)
Fe_1–N_1	1.962	2.097(3)	O_6–Fe_1–N_2	87.14	85.90(11)
Fe_1–N_2	1.962	2.114(3)	N_2–Fe_1–N_1	92.75	100.94(11)
N_1–C_1	1.473	1.473(5)	N_1–Fe_1–O_5	87.14	88.55(11)
N_1–C_3	1.300	1.293(4)	O_2–Fe_1–O_5	90.34	98.82(11)
N_2–C_{10}	1.473	1.478(5)	O_2–Fe_1–O_6	86.52	86.17(10)
N_2–C_{12}	1.300	1.289(4)	O_2–Fe_1–N_1	91.08	85.21(11)
O_2–C_9	1.306	1.313(4)	O_2–Fe_1–N_2	92.06	89.31(11)
O_4–C_{18}	1.306	1.318(4)	O_4–Fe_1–O_5	85.52	88.37(10)
O_5–C_{19}	1.275	1.277(5)	O_4–Fe_1–O_6	90.36	99.70(11)
O_6–C_{22}	1.275	1.284(5)	O_4–Fe_1–N_1	92.07	89.70(11)
			O_4–Fe_1–N_2	91.08	84.44(11)

modes are 1144 and 745 cm^{-1}, respectively, in good agreement with the reported values.

Catalytic reactivity

In order to evaluate the catalytic activity of this complex for the oxidation of sulfides, the reaction conditions were optimized with respect to the oxidation of methylphenyl sulfide (MPS) with respect to solvent, quantity of catalyst, and the amount of UHP.

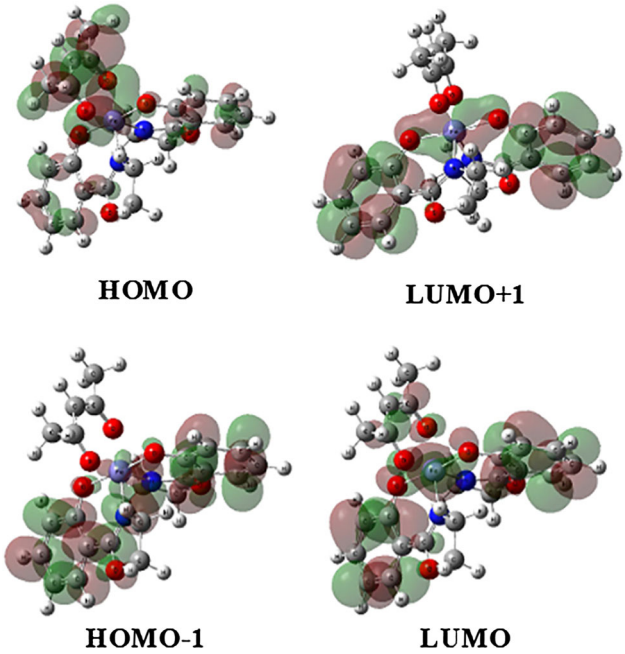

Fig. 3 Calculated HOMO−1, HOMO, LUMO, and LUMO+1 for the complex

Initially, oxidation of MPS was examined without catalyst and with either Fe(acac)$_3$ or [Fe(phox)$_2$(acac)]. As reported in Table 4, the maximum activity was observed with [Fe(phox)$_2$(acac)], whereas oxidation of MPS without catalyst gave almost no conversion. The conversion of MPS increased with increasing amount of catalyst from 0 to 0.01 mmol. When the amount of catalyst was further increased to 0.015 mmol, the selectivity for sulfoxide product was reduced from 96 to 89 %. Next, dichloromethane, chloroform, acetonitrile, acetone, methanol, and 1:1 mixtures of CH_2Cl_2/CH_3OH and CH_2Cl_2/CH_3CN were investigated as solvents. Among these choices, the 1:1 mixture of CH_3OH/CH_2Cl_2 was found to be the best for this protocol (Table 4). The amount of UHP also had a significant effect on both the conversion and methylphenyl sulfoxide selectivity (Table 4, entries 12–16). When the amount of UHP was increased from 0.1 to 0.4 mmol, the conversion of MPS increased drastically from 22 to 73 %. With a further increase in UHP to 0.5 mmol, the selectivity for methylphenyl sulfoxide decreased from 96 to 89 %, while the conversion of MPS increased from 73 to 80 %. In other words, the selectivity for sulfoxide would appear to be better for reactions with 2 equivalents of the oxidant compared to higher amounts.

In order to compare the present catalytic system with recently reported protocols, we compared the results obtained for MPS oxidations in the presence of other five-coordinated iron(III) complexes. As shown in Table 5, [Fe(phox)$_2$(acac)] gave lower oxidation yield but higher

Table 3 Experimental and calculated vibrational frequencies of the complex

Assignment	Experimental frequency (cm^{-1})	Calculated frequency	
		Unscaled (cm^{-1})	Scaled (cm^{-1})
α(C–H) $_{\text{benzene rings}}$	3150 (m)	3218–3177	3093–3054
α(C–H)$_{\text{phox, acac}}$		3157–3054	3035–2936
α(C=N)	1611 (s)	1675	1610
α_{asymm}(C–C)$_{\text{benzene rings}}$		1646	1582
α_{symm}(C–C)$_{\text{benzene rings}}$		1581	1520
α_{asymm}(C–C)$_{\text{acac}}$		1570	1509
δ(C–H)$_{\text{phox}}$		1551–1533	1491–1474
α_{asymm}(C–C)$_{\text{benzene rings}}$ + β(C–H)$_{\text{benzene rings}}$		1512	1453
δ(C–H)$_{\text{acac}}$		1508–1502	1450–1444
α_{asymm}(C–C)$_{\text{benzene rings}}$ + β(C–H)$_{\text{benzene rings}}$		1490	1432
α_{asymm}(C=O)$_{\text{acac}}$		1457	1401
α_{asymm}(C=O)$_{\text{oxazoline}}$	1368 (s)	1439	1383
α_{asymm}(C–C)$_{\text{benzene rings}}$ + α(C=O) $_{\text{benzene rings}}$ + bending of (C–H)$_{\text{phox}}$		1396	1342
α_{asymm}(C–C)$_{\text{benzene rings}}$ + α(C=O) $_{\text{benzene rings}}$ + bending of (C–H)$_{\text{phox}}$		1389	1335
β(C–H)$_{\text{benzene rings}}$		1190	1144
χ(C–H)$_{\text{phox}}$		1140	1096
γ(C–H)$_{\text{benzene rings}}$		775	745
α_{asymm}(Fe–O $_{\text{benzene rings}}$)	584 (w)	646	621
α_{symm}(Fe–O $_{\text{benzene rings}}$)	584 (w)	631	606
α_{symm}(Fe–O$_{\text{acac}}$)		451	434
α_{symm}(Fe–N)		399	384

α, stretching; β, in-plane bending; γ, out-of-plane bending; δ, scissoring; χ, rocking; band intensities are classified as strong (s), medium (m) or weak (w)

selectivity than the other complexes. Although the mechanism of these oxidation reactions is not yet known, it is probably related to the availability of a site for coordination of the substrate or oxo-intermediate in five-coordinated iron(III) complexes. Hence, the six-coordinated iron(III) complex [Fe(phox)$_2$(acac)] must gain a free site before the reaction can proceed.

The present complex [Fe(phox)$_2$(acac)] proved to be capable of catalyzing the oxidation of a range of structurally diverse sulfides (Table 6). Arylalkyl (Table 6, entries 1,2), arylbenzyl (Table 6, entry 3), dibenzyl (Table 6, entry 4), diaryl (Table 6, entry 5) and dialkyl (Table 6, entries 6–8) sulfides underwent clean and selective oxidation to the corresponding sulfoxide under air, with impressive selectivities. Very good conversions of substrates were obtained for all cases. Aromatic sulfides were found to undergo oxidation more easily than aliphatic substrates. In the case of dialkyl sulfides (Table 6, entries 6–8), no over-oxidation to the sulfone was observed.

In general, the reactivity of the catalytic system completely ceased after 15 min. Upon addition of UHP to a solution of the iron complex for the oxidation of methylphenyl sulfide, the absorption band at 230 nm assigned to LMCT [phenolate (p_π) → iron(III) ($d_{\sigma*}$)] [33, 34] of [Fe(phox)$_2$(acac)] disappeared gradually, and the solution turned from brown to pale yellow. The marked decrease in the absorption intensity at 230 nm after 15 min (Fig. 4) indicates the destruction of the catalyst, resulting in loss of reactivity. In the presence of greater amounts of the oxidant the decomposition of the catalyst increased, for example when a large excess of UHP (1 mmol) was added to the solution, the absorption band disappeared immediately and the brown solution became almost colorless.

Conclusions

The iron(III) complex [Fe(phox)$_2$(acac)] has been synthesized and characterized by physicochemical methods and by X-ray crystallography. The complex proved to be an effective catalyst for the oxidation of sulfides to their corresponding sulfoxides. However, the lack of a free site may explain the lower oxidation yields of the present complex compared to others reported previously. Nevertheless, easy preparation, mild reaction conditions, high yields of the products, short reaction times, and high

Table 4 The effect of various conditions in the oxidation of methylphenyl sulfide by [Fe(phox)$_2$(acac)]/UHP

Entry	Catalyst	Amount of catalyst (mmol)	Amount of UHP (mmol)	Solvent (1 mL)	Conversion (%) (TON)[a]	Selectivity to sulfoxide (%)[b]
1	–	–	0.4	CH_2Cl_2:CH_3OH	Trace	–
2	Fe(acac)$_3$	0.01	0.4	CH_2Cl_2:CH_3OH	54 (10.8)	98
3	Fe(phox)$_2$(acac)	0.01	0.4	CH_2Cl_2:CH_3OH	73 (14.6)	96
4	Fe(phox)$_2$(acac)	0.005	0.4	CH_2Cl_2:CH_3OH	48 (9.6)	99
5	Fe(phox)$_2$(acac)	0.015	0.4	CH_2Cl_2:CH_3OH	81 (16.2)	89
6	Fe(phox)$_2$(acac)	0.01	0.4	CH_2Cl_2	15 (3.0)	100
7	Fe(phox)$_2$(acac)	0.01	0.4	$CHCl_3$	13 (2.6)	100
8	Fe(phox)$_2$(acac)	0.01	0.4	CH_3CN	51 (10.2)	95
9	Fe(phox)$_2$(acac)	0.01	0.4	CH_3OH	44 (8.8)	99
10	Fe(phox)$_2$(acac)	0.01	0.4	CH_3COCH_3	39 (7.8)	98
11	Fe(phox)$_2$(acac)	0.01	0.4	CH_2Cl_2:CH_3CN	55 (11.0)	94
12	Fe(phox)$_2$(acac)	0.01	0	CH_2Cl_2:CH_3OH	Trace	–
13	Fe(phox)$_2$(acac)	0.01	0.1	CH_2Cl_2:CH_3OH	22 (4.4)	100
14	Fe(phox)$_2$(acac)	0.01	0.2	CH_2Cl_2:CH_3OH	35 (7.0)	100
15	Fe(phox)$_2$(acac)	0.01	0.3	CH_2Cl_2:CH_3OH	51 (10.2)	97
16	Fe(phox)$_2$(acac)	0.01	0.5	CH_2Cl_2:CH_3OH	80 (16.0)	89

[a] TON = (mmol of sulfoxide + mmol of sulfone)/mmol of catalyst

[b] Selectivity to sulfoxide = (sulfoxide %/(sulfoxide % + sulfone %)) × 100

Table 5 Recently reported catalytic systems for oxidation of sulfides by Fe(III) complexes[a]

Entry	Catalyst	Conversion (%)	Selectivity (%)	References
1	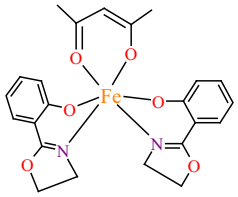	73	96	Present work
2	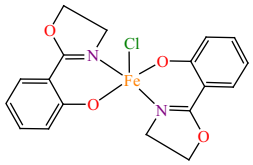	83	92	[18]
3	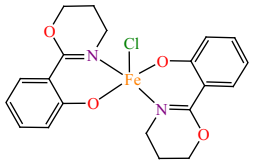	85	86	[19]
4	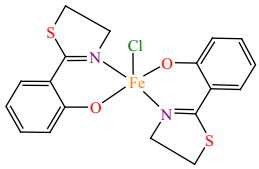	91	86	[20]

[a] Reaction conditions: 1 mol % of catalyst, 0.4 mmol UHP, 1 mL of CH_2Cl_2/CH_3OH/rt/15 min

Table 6 Oxidation of sulfides catalyzed by $[Fe(phox)_2(acac)]/UHP$[a]

Entry	Substrate	Conversion (%)[b] (TON)[c]	Selectivity (%)[d]
1	PhSMe	73 (14.6)	96
2	PhSEt	70 (14.0)	96
3	$PhSCH_2Ph$	74 (14.8)	95
4	$PhCH_2SCH_2Ph$	81 (16.2)	91
5	Ph_2S	72 (14.4)	98
6	Et_2S	41 (8.2)	100
7	Bu_2S	35 (7.0)	100
8	$(C_8H_{17})_2S$	33 (6.6)	100

[a] The molar ratios for $[Fe(phox)_2(acac)]$/substrate/oxidant were 1:20:40. The reactions were performed in a (1:1) mixture of CH_2Cl_2/CH_3OH (1 mL) under air at room temperature

[b] The GC yields (%) are reported relative to the starting sulfide

[c] TON = (mmol of sulfoxide + mmol of sulfone)/mmol of catalyst

[d] Selectivity to sulfoxide = (sulfoxide %/(sulfoxide % + sulfone %)) × 100

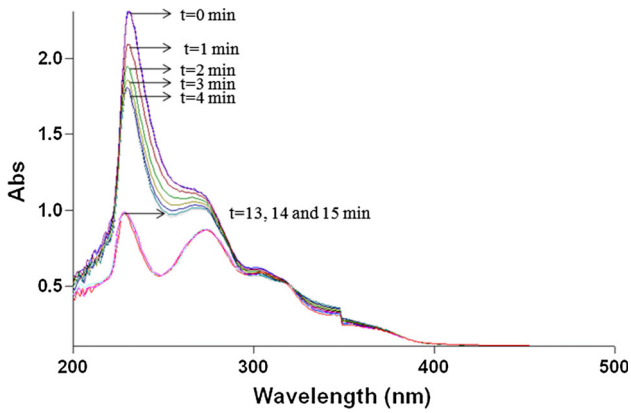

Fig. 4 Changes of the absorption at 320 nm of $[Fe(phox)_2(acac)]$ in oxidation of methylphenyl sulfide after addition of UHP

selectivity make this catalytic system of potential interest for oxidation reactions.

Supplementary data

The CIF file of crystal structure complex $[Fe(phox)_2(acac)]$ has been deposited with the CCDC, No.1030742. This data can be obtained free of charge via http://www.ccdc.cam.ac.uk/conts/retrieving.html, or from the Cambridge Crystallographic Data Centre, 12 Union Road, Cambridge CB2 1EZ, UK; fax: (+44) 1223-336-033; or e-mail: deposit@ccdc.cam.ac.uk

Acknowledgments Authors thank the Research Council of the University of Maragheh (M.A), Semnan University (A. A), and the National Science Foundation (L.K.W) for funding of this work.

References

1. Amini M, Haghdoost MM, Bagherzadeh M (2014) Coord Chem Rev 268:83–100
2. Amini M, Haghdoost MM, Bagherzadeh M (2013) Coord Chem Rev 257:1093–1121
3. Jeyakumar K, Chakravarthy RD, Chand DK (2009) Catal Commun 10:1948–1951
4. Muthupandi P, Alamsetti SK, Sekar G (2009) Chem Commun 2009:3288–3290
5. Comba P, Lee Y-M, Nam W, Waleska A (2014) Chem Commun 50:412–414
6. Hong D, Mandal S, Yamada Y, Lee Y-M, Nam W, Llobet A, Fukuzumi S (2013) Inorg Chem 52:9522–9531
7. Bayat A, Shakourian-Fard M, Ehyaei N, Hashemi MM (2014) RSC Adv 4:44274–44281
8. Bagherzadeh M, Amini M (2009) Inorg Chem Commun 12:21–25
9. Hussain SMS, Ibrahim MB, Fazal A, Suleiman R, Fettouhi M, Ali BE (2014) Polyhedron 70:39–46
10. Amini M, Bagherzadeh M, Moradi-Shoeili Z, Boghaei DM, Ellern A, Woo LK (2013) J Coord Chem 66:464–472
11. Chen M-T, Chang P-J, Huang C-A, Peng K-F, Chen C-T (2009) Dalton Trans 2009:9068–9074
12. Bagherzadeh M, Amini M, Ellern A, Woo LK (2012) Inorg Chim Acta 383:46–51
13. Amini M, Bagherzadeh M, Atabaki B, Derakhshandeh PG, Ellern A, Woo LK (2014) J Coord Chem 67:1429–1436
14. Hoogenraad M, Ramkisoensing K, Driessen WL, Kooijman H, Spek AL, Bouwman E, Haasnoot JG, Reedijk J (2001) Inorg Chim Acta 320:117–126
15. Ene CD, Lungu A, Mihailciuc C, Hillebrand M, Ruiz-Perez C, Andruh M (2012) Polyhedron 31:539–547
16. Jaworska M, Stopa G, Stasicka Z (2010) Nitric Oxide 23:227–233
17. Conradie MM, van Rooyen PH, Conradie J (2013) J Mol Struct 1053:134–140
18. Amini M, Arab A, Derakhshandeh PG, Bagherzadeh M, Ellern A, Woo LK (2014) Spectrochim Acta A Mol Biomol Spectrosc 133:432–438
19. Amini M, Haghdoost MM, Bagherzadeh M, Ellern A, Woo LK (2013) Polyhedron 61:94–98
20. Amini M, Bigdeli M, Delsouz-Hafshejani S, Ellern A, Woo LK (2014) Z Anorg Allg Chem 640:385–389
21. Hoveyda HR, Kamnaname V, Rettig SJ, Orvig C (1992) Inorg Chem 31:5408–5416
22. Frisch MJ (2003) Gaussian 03 Revision B 03. Gaussian Inc, Pittsburgh, PA
23. Maurya MR, Dhaka S, Avelilla F (2014) Polyhedron 67:145–159
24. Crichton RR (2008) Biological inorganic chemistry, an introduction, vol 1. Elsevier, Amsterdam, The Netherlands
25. Bhattacharjee CR, Goswami P, Pramanik HAR, Paul PC, Mondal P (2011) Spectrochim Acta A Mol Biomol Spectrosc 78:1408–1415
26. Koner S, Iijima S, Mizutani F, Harata K, Watanabeb M, Nagasawa A, Sato M (1999) Polyhedron 18:2201–2204
27. Cappelli C, Duce C, Formica M, Fusi V, Ghezzi L, Giorgi L, Micheloni M, Paoli P, Rossi P, Rosaria Tine M (2014) Inorg Chim Acta 417:230–238
28. Qu Y (2012) Spectrochim Acta A Mol Biomol Spectrosc 94:205–209
29. Sayin K, Karakas D (2014) J Mol Struct 1076:244–250
30. Foresman JB, Frisch A (1996) Exploring chemistry with electronic structure methods, 2nd edn. Gaussian Inc., Pittsburgh, PA

31. Rastogi VK, Palafox MA, Tanwar RP, Mittal L (2002) Spectrochim Acta A Mol Biomol Spectrosc 58:1987–2004
32. Bellamy LJ (1975) The infrared spectra of complex molecules, 3rd edn. Wiley, New York
33. Shongwe MS, Al-Rashdi BA, Adams H, Morris MJ, Mikuriya M, Hearne GR (2007) Inorg Chem 46:9558–9568
34. Davis MI, Orville AM, Neese F, Zaleski JM, Lipscomb JD, Solomon EIJ (2002) J Am Chem Soc 124:602–614